ELSEVIER

7 November 1997

Chemical Physics Letters 279 (1997) 92–99

CHEMICAL PHYSICS LETTERS

Particle size dependent CO dissociation on alumina-supported Rh: a model study

M. Frank [a], S. Andersson [b], J. Libuda [a], S. Stempel [a], A. Sandell [c], B. Brena [b], A. Giertz [b], P.A. Brühwiler [b], M. Bäumer [a], N. Mårtensson [b], H.-J. Freund [a]

[a] *Fritz-Haber-Institut der Max-Planck-Gesellschaft, Faradayweg 4–6, D-14195 Berlin, Germany*
[b] *Department of Physics, Uppsala University, Box 530, S-751 21 Uppsala, Sweden*
[c] *Department of Synchrotron Radiation Research, Lund University, Box 118, S-221 00 Lund, Sweden*

Received 23 June 1997; in final form 25 September 1997

Abstract

Via deposition of Rh from the gas phase onto a thin, well-ordered alumina film we have prepared various of alumina-supported Rh particle systems. The morphologies and particle sizes have been characterised with spot profile analysis LEED and STM measurements. The probabilities for thermally induced dissociation of adsorbed CO at temperatures between 350 and 500 K were determined from C 1s photoelectron spectra. For small aggregates the dissociation activity increases with increasing average particle size. After reaching a maximum for particles containing an average of 500 to 1000 Rh atoms, the fraction of dissociated CO decreases to values closer to those observed on well-prepared Rh single crystal surfaces. © 1997 Published by Elsevier Science B.V.

1. Introduction

In dispersed metal catalysts one makes use of the unique chemical properties of an ensemble of small metal particles anchored to a support [1]. Many attempts have been undertaken to uncover the reasons for their catalytic behaviour [2]. Several issues have emerged from previous investigations, one of which we want to briefly address in our study:

- Is the particular size or morphology of the deposited particle relevant in optimising the rate of a given chemical reaction?

In the past, transmission electron microscopy [3] as well as extended X-ray absorption fine structure analysis [4] have been successfully applied to study the morphology and structure of dispersed metal catalysts. Recently, these investigations have been complemented by studies on model systems. These model catalysts consist of a single crystal substrate or a thin film (often an oxide), onto which metals are usually evaporated under control of substrate temperature and metal vapour flux [5,6]. This allows the preparation of relatively narrow particle size distributions. Scanning probe techniques as well as electron diffraction may be applied in a straightforward fashion to the thin film systems in order to determine the size, shape and height of the metal particles and, from the island density, also the number of atoms per island [7,8]. Since the model systems are being prepared under ultrahigh vacuum conditions, the chemical composition of the substrate is under control. For example, oxide substrates with high crystallographic

0009-2614/97/$17.00
PII S0009-2614(97)01114-7

order and without the presence of hydroxyl groups or carbon at the surface may be prepared [9,10]. This situation is not easily achieved for real catalysts. The model system therefore allows us to explore a limiting case and compare it with the real systems.

We have chosen to investigate a certain chemical reaction, namely the dissociation of CO on alumina-supported Rh as a function of particle size. The Rh/Al_2O_3 system has been extensively studied in the past. In addition, experiments on compact and stepped Rh single crystal surfaces are available. While on the dispersed catalyst systems CO dissociation takes place above room temperature [11,12], close-packed Rh single crystal surfaces adsorb and desorb CO reversibly [13–16]. Only on some stepped metal single crystals [17–20] and on defective Rh surfaces [21,22] has CO dissociation been observed. The precise nature of the step sites required for dissociation, however, is still unclear.

The results of the few studies that have addressed the question on how the dissociation activity depends on Rh particle size have been controversial. On the basis of a TEM investigation coupled with SIMS and TPD measurements, Matolín et al. come to the conclusion that the fraction of dissociated CO decreases with increasing cluster size [23,24]. In this case, however, two different oxide substrates were used. Later, Nehasil et al., also basing their investigation on TPD, found the opposite trend for alumina-supported Rh [25]. We have recently published a preliminary study on a Rh/Al_2O_3 model system presenting evidence for an increased dissociation rate with increasing island size [26]. Our analysis was based upon the combination of electron diffraction, TPD and photoelectron spectroscopy. The island diameters investigated in the latter study ranged from 5 to 30 Å, thus covering a fairly wide range of particle sizes. While the spectroscopic evidence for a rate increase was clear, the problem remains as to how this observation allows us to make connections to the much lower single crystal activities. We have therefore studied an even wider range of island sizes using preparation of the dispersed metal system at low and high temperatures and characterising the morphology by spot profile analysis–LEED (SPA–LEED) and STM.

We found that the dissociation probability goes through a maximum and declines again. The maximum is rather wide and is connected with islands containing several hundred atoms. This indicates that the particle morphology, rather than the unique electronic structure, of an aggregate of particular size is responsible for the increase in dissociation rate.

2. Experimental

The experiments were performed in several ultra-high vacuum systems. X-ray photoelectron (XP) spectra were recorded at beamline 22 at the Swedish synchrotron radiation facility MAX-lab (Lund). Here, the apparatus contains a modified Zeiss SX-700 monochromator in conjunction with a large hemispherical electron energy analyser [27]. The C 1s spectra were taken with a total resolution of 0.4 eV. All XPS binding energies are referred to the Fermi level of the NiAl(110) substrate. Absolute photon energies were determined using photoemission spectra excited by first- and second-order radiation. The crystal was mounted in a wire loop which allowed resistive heating, while the sample temperature was measured with a NiCr/Ni thermocouple spot welded to the crystal.

STM images were taken with a room-temperature AFM/STM (Omicron). The sample was mounted on a small molybdenum plate allowing transfer from the preparation stage to the microscope. These structural investigations were complemented by SPA–LEED measurements in a third chamber.

The alumina film was prepared via oxidation of a clean NiAl(110) single crystal surface according to a procedure similar to the one reported previously [9]. As opposed to the NiAl surface, at 90 K no CO adsorbs on the oxide film. Thus, the quality of the oxide could be assessed from the absence of a C 1s signal after dosage of CO at 90 K. Alternatively, STM images or LEED spot profiles were taken for this purpose.

Rh metal (Heraeus, $> 99.9\%$) was evaporated from a rod via electron bombardment. During evaporation the sample was put in a retarding potential to avoid effects due to Rh ions being accelerated towards the sample. A calibration of the metal flux was obtained by a quartz crystal microbalance. The deposition rates varied between 0.6 and 1.0 Å min^{-1} (1 Å Rh corresponds to 7.3×10^{14} cm^{-2}).

3. Results and discussion

Rh deposits have been prepared by evaporation from an oven onto a thin, well-ordered alumina film grown on a NiAl(110) single crystal. The properties of the oxide film are described elsewhere [9,28]. Fig. 1 shows large-area STM images of the Al_2O_3 surface after exposure to Rh at 90 and 300 K. The growth mode of Rh on our substrate is of Volmer–Weber type in both cases. However, while at low temperature the distribution of islands on the oxide surface is random, at room temperature heterogeneous nucleation at the characteristic domain boundary network of the alumina film dominates [29]. Most prominent are the straight antiphase domain boundaries which cut each of the two rotational domains of the oxide film into parallel stripes with an average width of ~ 120 Å [28]. In the close up of the 90 K deposit (Fig. 2a), these boundaries appear as line protrusions (arrow). The additional fine structure represents the electronic structure of the hexagonal Al_2O_3 surface [28]. The close up of the room-temperature deposit (Fig. 2b) shows the presence of individual islands which do not coalesce to form a metal wire. An explanation for this observation may be found by resorting to results obtained for Pt, Pd and Ta deposits on the same substrate [30]. We have found indications from transmission electron microscopy that the lattice of the deposited metal particles is considerably strained due to the strong interaction of the metals with the oxide substrate. Therefore, island coalescence may be unfavourable at the given temperatures.

Concerning the morphology of the Rh aggregates, we have concluded from SPA–LEED as well as from STM measurements that the particles are mostly disordered, i.e. most of them are non-crystalline [29]. For the room-temperature deposits, however, at large metal exposures a fraction of the particles evolve straight edges and a flat top. Their triangular shape is consistent with Rh crystallites exposing mainly (111) facets. In addition, from STM images (and in the

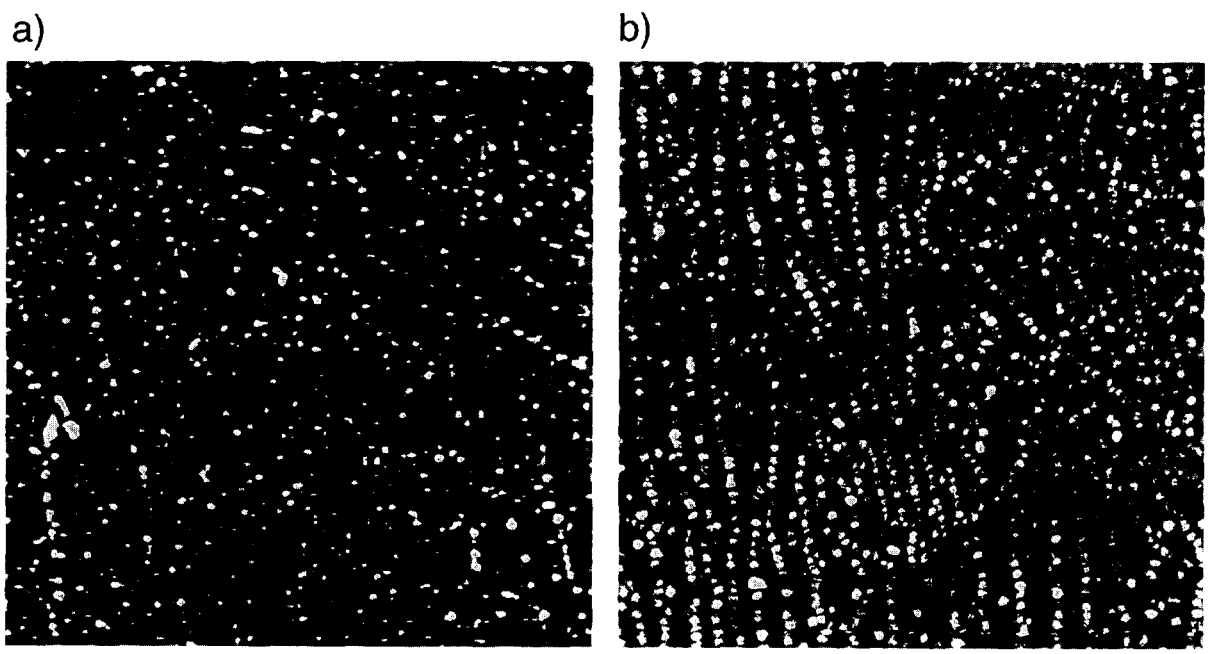

Fig. 1. STM overview images: (a) 0.1 Å Rh deposited at 90 K, 1900 Å × 1900 Å (CCT, $U = +5.1$ V, $I = 2.0$ nA) and (b) 5.0 Å Rh deposited at 300 K, 3000 Å × 3000 Å (CCT, $U = +1.0$ V, $I = 1.3$ nA).

case of the 90 K deposits also via SPA–LEED) we have determined the island density over a wide range of metal exposures. From this, the average number of atoms constituting the islands can be calculated.

Summarising the morphology studies, we have demonstrated that individual Rh particles of variable average size may be prepared. Also, our LEED data do not indicate any significant coalescence upon elevating the temperature. We now turn to the reactivity studies.

After metal growth, the absence of both CO and atomic carbon was checked via XPS. Then, 40 L CO were dosed at a sample temperature of 90 K. Fig. 3 shows a series of C 1s spectra taken at 90 K after successive heating steps. The average island size amounts to ~ 10 000 atoms. At 90 K a strong signal at 285.8 eV typical for molecularly-adsorbed CO is observed. The peak is not symmetrical and the lineshape appears to change prior to the emergence of another signal at 350 K. At a substrate temperature of 500 K only the second peak remains. Its position is fully compatible with atomic carbon in its carbidic form, as is expected if the feature is due to atomic carbon stemming from CO dissociation. In fact, the absence of any molecularly-adsorbed CO has been checked by X-ray absorption spectroscopy where the lack of the C 1s $\rightarrow 2\pi *$ absorption is fully compatible with the above statement [31]. We would like to note that the presence of some atomic carbon immediately after gas dosage at 90 K might point to the existence of catalytically active sites dissociating CO at low temperatures.

If we now integrate the signal caused by molecular CO at 90 K, we determine the amount of adsorbed CO molecules. Similarly, integration of the signal corresponding to carbidic carbon at high temperatures allows us to determine the quantity of dissociated CO. The ratio is equivalent to the probability that molecular CO dissociates on a given sample. This quantification requires photoelectron diffraction effects to be small, which should be best fulfilled for the disordered low-temperature deposits.

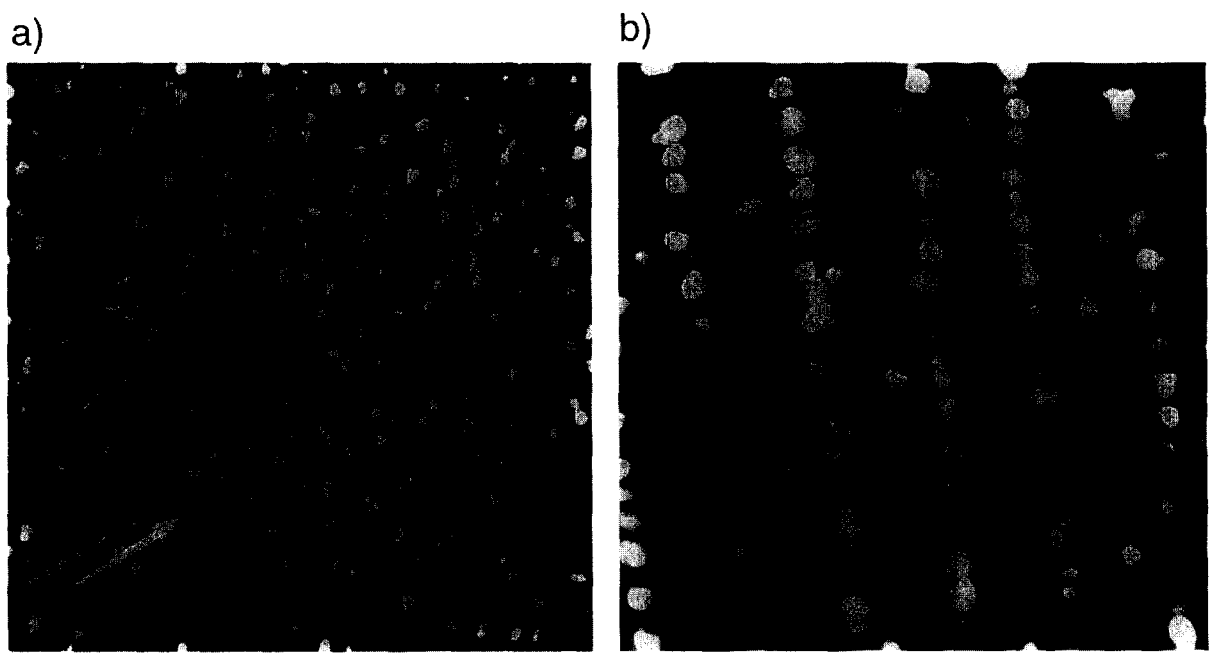

Fig. 2. STM close-ups: (a) 0.1 Å Rh deposited at 90 K, 800 Å × 800 Å (CCT, $U = +5.1$ V, $I = 2.0$ nA) and (b) 5.0 Å Rh deposited at 300 K, 1000 Å × 1000 Å (CCT, $U = +0.9$ V, $I = 1.2$ nA). The line protrusions (arrow) are antiphase domain boundaries of the oxide film.

Series of spectra similar to the one shown in Fig. 3 have been recorded for eleven different deposits with varying island sizes. Four of these were prepared by evaporating Rh at 90 K (metal exposures between 0.6 and 12 Å) and seven by deposition at 300 K (metal exposures between 0.5 and 64 Å). In Fig. 4, the C 1s spectra representing the initial state ($T = 90$ K) of molecular CO and the final state ($T = 600$ K) of dissociated CO have been superimposed.

Preliminary results on the low-temperature metal deposits have been reported earlier [26]. These samples represent aggregates consisting of less than ~ 800 atoms. As mentioned in Section 1, the probability for CO dissociation increases with particle size as revealed by the rise in relative intensity of the C 1s signal at 284 eV. Rh deposition at room temperature allows us to access larger islands containing more than 1000 atoms, as well as the range of sizes that can be prepared at low temperature. Thus the consistency of the present data with the previously published results can be checked. Clearly, considering the relative intensities of molecular and atomic C 1s peaks, a quick inspection of Fig. 4 shows that the rise in dissociation probability with increasing island size observed for the low-temperature preparation is reversed for larger aggregates. This becomes more apparent if we perform a quantitative analysis of the peak intensities.

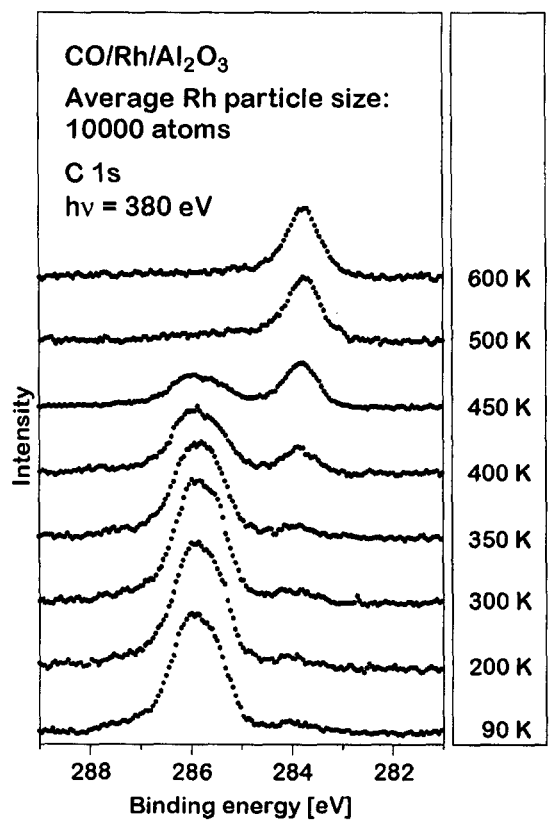

Fig. 3. Series of C 1s photoelectron spectra taken after deposition of 16 Å Rh at room temperature, dosage of 40 L CO at 90 K and subsequent heating to the indicated temperatures.

In Fig. 5 the C 1s intensity due to thermally dissociated CO relative to the total low-temperature C 1s signal is plotted as a function of Rh particle size. The amount of atomic carbon present immediately after CO dosage is indicated as well. The trend deduced by inspection of Fig. 4 is confirmed by the quantitative analysis. Small particles containing ~ 100 atoms exhibit a low tendency to dissociate CO, while for the larger particles the probability for dissociation increases up to the point where the aggregates contain ~ 1000 atoms. Beyond this size the dissociation activity declines and reaches a value closer to either the small Rh clusters or the stepped Rh single crystal surfaces. For comparison, we have used the value reported by Rebholz et al. [19] for CO dissociation on the Rh(210) surface. As mentioned above, smooth close-packed single crystal Rh surfaces do not dissociate CO.

The obvious questions are, why does the CO dissociation activity increase as a function of particle size, and why does it proceed through a maximum for a range of larger cluster sizes and subsequently drop to a lower value?

In an attempt to answer these questions we note that small unsupported Rh cluster ions up to Rh_{14} only adsorb CO molecularly without dissociation, as recently shown by Irion and coworkers [32]. The smallest aggregates we have been able to investigate via photoelectron spectroscopy with an acceptable signal-to-noise ratio contain ~ 45 atoms and do dissociate some CO. It is possible that for particles consisting of less than 20 atoms the CO dissociation activity is negligible but it is even more likely that the interaction between the aggregate and the support changes the electronic structure of the aggregate with respect to the unsupported situation. There are indications for such strong interactions with the substrate. STM images show that the smallest particles

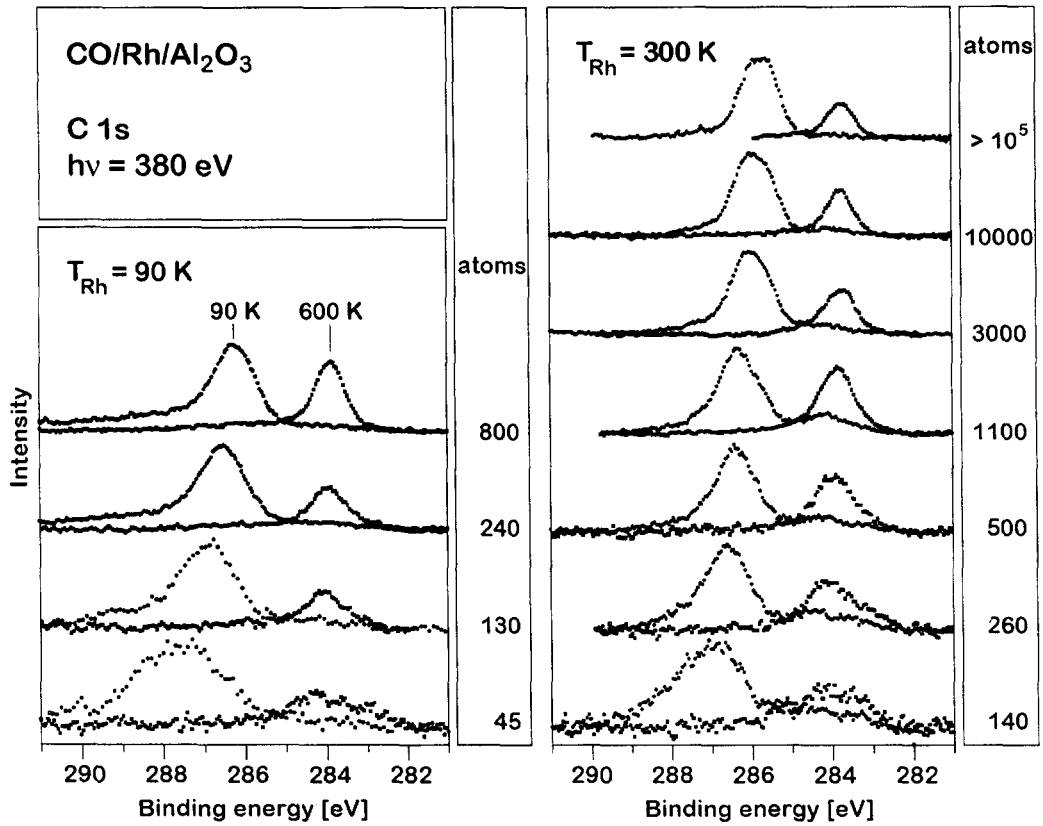

Fig. 4. C 1s photoelectron spectra of CO on Rh deposits evaporated at sample temperatures of 90 K (left) and 300 K (right), before and after heating. The mean number of Rh atoms per island is given next to the corresponding spectra.

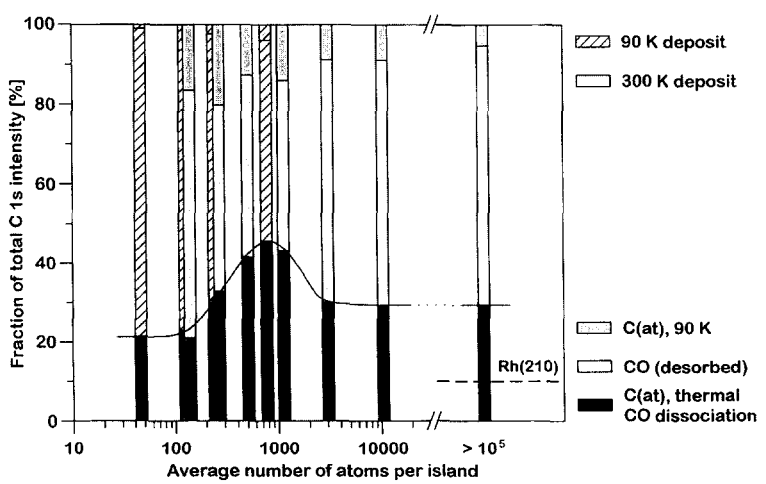

Fig. 5. Relative C 1s peak intensities of thermally dissociated CO after heating the sample to 600 K (bottom) and of atomic carbon present at 90 K (top) as a function of Rh particle size. 100% correspond to the total C 1s intensity at 90 K. For comparison, the fraction of CO dissociated on Rh(210) is indicated with a dashed line [19].

grow as flat single metal layers in intimate contact with the oxide. The aggregates imaged in Fig. 2a, for example, exhibit an average Rh aggregate height of ~ 3 Å, compatible with a single layer. When more Rh is evaporated the height of the particles increases, and when the particle size exceeds several hundred atoms, the dissociation probability increases towards the maximum. We therefore feel that the activity for dissociation is connected with particle morphology. Obviously, as known from single crystal surfaces, steps at the surface may induce dissociation. As soon as the aggregates consist of more than a single or a double metal layer, the ability for the particle to accommodate steps increases. In fact, the density of steps on a given aggregate will rise until a particular size of the aggregate is reached, a critical radius so to speak, which may depend on the degree of metal surface interaction and metal cohesive energy. After this size and shape has been reached the aggregates will tend to form regular shapes which contain a considerably smaller number of steps, finally exposing facets resembling single crystal surfaces. These changes in morphology then are also responsible for the observed reactivities.

In addition, a steric argument may become important for small aggregates. CO needs at least two well-separated sites into which the released carbon and oxygen atoms can be accommodated and, therefore, a sufficiently large Rh ensemble is needed in order for dissociation to occur [33,34]. Taking the limited size of the smallest particles into account, it is quite conceivable that on these there is simply not sufficient space to accommodate a large concentration of dissociation products. In the future it may be possible to obtain more detailed information on the structure of the dissociation products from scanning probe microscopy.

A more detailed picture of the mechanism of CO dissociation, in particular concerning changes in bonding characteristics before dissociation, emerges from a more sophisticated analysis of the photoelectron spectra [35]. Briefly, C 1s spectra taken at high resolution show that the CO-related signal consists of two components, indicating the presence of different CO species. Upon heating to 300 K, intensity is transferred between the components. The extent of this process is closely correlated with the amount of CO dissociated at higher temperatures. This points to a partial rearrangement of the CO molecules from sites with lower metal coordination into more highly coordinated sites where they dissociate upon further heating. This will be discussed in detail in a separate paper [35].

4. Conclusions

The probability for CO dissociation on alumina-supported Rh increases with increasing particle size for small and medium-sized clusters. This is possibly due to the rather strong interaction with the oxide support. The dissociation probability goes through a maximum for aggregates containing up to 1000 atoms after which it decreases until it reaches a value closer to activities of stepped single crystal surfaces. The correlation to the development of particle height with the number of atoms per island suggests that this may be connected with the morphology of the aggregates. It is conceivable that a particular range of particle sizes may stabilise an especially high density of steps which in turn leads to the observed high dissociation activity. This range of aggregate sizes is influenced, among other factors, by the metal substrate interaction as well as by the metal cohesive energy.

Our study shows that for certain reactions relatively large particle sizes may be relevant. These are beyond those intended to be produced via mass-selection prior to deposition. However, the question as to whether the substrate influences the reactivity of small clusters may be effectively tackled by mass-selective deposition.

The present study might also provide an explanation for the two contradictory observations in the literature which report both an increase and a decrease in CO dissociation probability [23–25]. These studies might probe the situation on different sides of our maximum. Alternatively, the variation of the oxide substrate could result in a modified reactivity due to changes in metal–support interaction and particle orientation.

Acknowledgements

We thank the staff at MAX-lab for invaluable experimental assistance. This work was supported by

Deutsche Forschungsgemeinschaft, Ministerium für Wissenschaft und Forschung des Landes Nordrhein-Westfalen, Fonds der Chemischen Industrie and by the Swedish Materials Research Consortium on Clusters and Ultrafine Particles, which is funded by the Swedish National Board for Industrial and Technical Development (NUTEK) and the Swedish Natural Science Research Council (NFR). MF and JL thank the Studienstiftung des deutschen Volkes for fellowships.

References

[1] A.B. Stiles (Ed.), Catalyst Supports and Supported Catalysts, Butterworth, Boston, MA, 1987.
[2] R.M. Lambert, G. Pacchioni (Eds.), Chemisorption and Reactivity on Supported Clusters, Thin Films, NATO (N. Atlantic Treaty Org.) ASI (Adv. Stud. Inst.) Ser., Ser. E, Vol. 331, Kluwer, Dordrecht, 1997.
[3] A.K. Dayte, D.J. Smith, Catal. Rev. — Sci. Eng. 34 (1992) 129.
[4] J.H. Sinfelt, G.H. Via, F.W. Lytle, Catal. Rev. — Sci. Eng. 26 (1984) 81.
[5] D.W. Goodman, Chem. Rev. 95 (1995) 523.
[6] H.-J. Freund, Angew. Chem., Int. Ed. Engl. 36 (1997) 452.
[7] M. Bäumer, J. Libuda, A. Sandell, H.-J. Freund, G. Graw, Th. Bertrams, H. Neddermeyer, Ber. Bunsenges. Phys. Chem. 99 (1995) 1381.
[8] C. Xu, D.W. Goodman, Chem. Phys. Lett. 263 (1996) 13.
[9] R.M. Jaeger, H. Kuhlenbeck, H.-J. Freund, M. Wuttig, W. Hoffmann, R. Franchy, H. Ibach, Surf. Sci. 259 (1991) 235.
[10] P.J. Chen, D.W. Goodman, Surf. Sci. 312 (1994) L767.
[11] F. Solymosi, A. Erdöhelyi, Surf. Sci. 110 (1981) L630.
[12] A. Erdöhelyi, F. Solymosi, J. Catal. 84 (1983) 446.
[13] D.G. Castner, B.A. Sexton, G.A. Somorjai, Surf. Sci. 71 (1978) 519.
[14] L.H. Dubois, G.A. Somorjai, Surf. Sci. 91 (1980) 514.
[15] J.T. Yates Jr., E.D. Williams, W.H. Weinberg, Surf. Sci. 91 (1980) 562.
[16] L.A. DeLouise, N. Winograd, Surf. Sci. 138 (1984) 417.
[17] R.A. Marbrow, R.M. Lambert, Surf. Sci. 67 (1977) 489.
[18] D.G. Castner, G.A. Somorjai, Surf. Sci. 83 (1979) 60.
[19] M. Rebholz, R. Prins, N. Kruse, Surf. Sci. Lett. 259 (1991) L797.
[20] M. Rebholz, R. Prins, N. Kruse, Surf. Sci. 269/270 (1992) 293.
[21] B.A. Sexton, G.A. Somorjai, J. Catal. 46 (1977) 167.
[22] D.G. Castner, L.H. Dubois, B.A. Sexton, G.A. Somorjai, Surf. Sci. 103 (1981) L134.
[23] V. Matolín, M.H. Elyakhloufi, K. Mašek, E. Gillet, Cat. Lett. 21 (1993) 175.
[24] V. Matolín, K. Mašek, M.H. Elyakhloufi, E. Gillet, J. Catal. 143 (1993) 492.
[25] V. Nehasil, I. Stará, V. Matolín, Surf. Sci. 331/333 (1995) 105.
[26] J. Libuda, M. Frank, A. Sandell, S. Andersson, P.A. Brühwiler, M. Bäumer, N. Mårtensson, H.-J. Freund, in: A. Okiji, H. Kasai, K. Makoshi (Eds.), Elementary Processes in Excitations and Reactions on Solid Surfaces, Springer Series in Solid State Sciences, vol. 121, Springer, Berlin, 1996, p.210.
[27] J.N. Andersen, O. Björneholm, A. Sandell, R. Nyholm, J. Forsell, L. Thånell, A. Nilsson, N. Mårtensson, Synch. Radiat. News 4 (1991) 15.
[28] J. Libuda, F. Winkelmann, M. Bäumer, H.-J. Freund, Th. Bertrams, H. Neddermeyer, K. Müller, Surf. Sci. 318 (1994) 61.
[29] M. Bäumer, M. Frank, J. Libuda, S. Stempel, H.-J. Freund, Surf. Sci. (in press).
[30] M. Klimenkov, S. Nepijko, H. Kuhlenbeck, M. Bäumer, R. Schlögl, H.-J. Freund, Surf. Sci. (in press).
[31] J. Libuda, Dissertation, Ruhr-Universität, Bochum, 1996, p.123.
[32] M.P. Irion, private communication.
[33] A. de Koster, R.A. van Santen, Surf. Sci. 233 (1990) 366.
[34] W.M.H. Sachtler, M. Ichikawa, J. Phys. Chem. 90 (1986) 4752.
[35] S. Andersson, M. Frank, A. Sandell, J. Libuda, A. Giertz, B. Brena, P.A. Brühwiler, M. Bäumer, N. Mårtensson, H.-J. Freund, J. Chem. Phys. (submitted).